SPIRE

Astronomical Calibration Sources for Herschel-SPIRE

Prepared by: **Peter Hargrave**

Document number: **SPIRE-UCF-NOT-003016**

Issue: **Version 0.1** **Date:** **8th April 2008**

Contents

1 Introduction

This note summarizes the astronomical sources to be used for calibration (flux and pointing) of Herschel-SPIRE.

2 Calibration source requirements

2.1 Photometer

- Point-like in 18” beam
- Bright – well above confusion limit, >~100mJy
- Not too bright - <~200Jy
- Non-variable, or known variability
- Good sky distribution & Herschel visibility
- Well modelled/known SEDs, with in-band accuracies > SPIRE requirement (10%)
    - No line contamination is desirable.

2.2 Spectrometer

In addition to the requirements for the photometer sources:-

- Line fluxes accurately known or predicted
- Several observable lines
- Lines must be well isolated – coverage of FTS dynamic range

3 Observing bright sources

There will be times when it is desirable/necessary to use a bright source (e.g. Uranus) as a calibration target. Above some flux level, the detector response will enter a non-linear regime. However, this response is well-understood, and can easily be corrected for. More of a problem is the limited dynamic range for a single observation imposed by the level at which the ADC’s will saturate. Currently modelled best (worst) case dynamic range is 300 (50) Jy, depending on detector parameters, background level etc. The limited dynamic range can be addressed by adjusting the detector bias to reduce responsivity. For instance, increasing the bias by a factor of ~3 can double the dynamic range. Further analysis is needed to define the limiting source brightness for the FTS.

4 Photometer calibration – wavelength definition and colour correction.

The standard photometer product will be flux densities, quoted at wavelengths of 250, 350 and 500μm. The pipeline must make some standard assumptions about the source spectrum. The pipeline will assume that the source spectrum varies across the band as ν^{-1}, i.e. making α_s = -1 in equation (1), below,

$$S_S(\nu) = S_S(\nu_o)\left(\frac{\nu}{\nu_o}\right)^{\alpha_S} \qquad 1$$

where $S_S(\nu)$ is the signal variation with frequency, ν and ν_o is the central frequency of the band at which the flux is quoted.

5 Routine calibration philosophy

We aim to observe fewer, well-known sources many times, rather than many different sources. With this in mind, we have designated sources as primary, secondary and tertiary, and will always try to observe primary and secondary sources, in preference to tertiary sources.

PCal will be used to transfer and monitor the calibration from one observation to the next.

6 Classification of calibration sources

Ideally, we would have a selection of sources whose in-band fluxes are known to high accuracy, that cover a range of flux densities from a few 100mJy to ~300Jy. Unfortunately, compromises have to be made. Of highest priority is the predicted photometric flux error, and this is what largely governs the classification of the sources.

6.1 Primary sources

These sources should be very well-known, with robust and well-tested models. Predicted flux errors should be <5% (TBD) in the SPIRE bands.

6.2 Secondary sources

Secondary sources have been listed where there is sufficient confidence that we could obtain photometric flux errors <~10% either now, or imminently with further modelling/observations of that source. These sources could be variable (e.g. asteroids), as long as the variability is well-known, and the flux modelled at the calibration observation epoch. They could also be slightly extended (e.g. planetary nebulae), as long as a beam correction is made. Included in this list are stellar sources. These sources are at the lower end of the SPIRE flux density range, and therefore very useful for calibrating observations of faint sources. However, in most cases, observations are needed in the sub-mm to fully constrain the SED's, and reduce the errors in the flux prediction for the SPIRE bands.

6.3 Tertiary sources

This list includes objects where the flux predictions are more uncertain, but could prove useful sources once further observations have been made, and models refined.

7 General notes

7.1 Source visibility

Visibility information for all sources listed in this document is stored in a Microsoft project file "sources-timeline2.mpp". This file will be the main calibration observation planning tool. It contains all information about source visibility and observing constraints (proximity to other sources, etc), as well as flux estimates for that observing period, and any relevant literature for that source.

7.2 Visibility plots

For all calibration sources, there are three types of plot presented, which shall be described below:-

- Solar elongation vs. date.
    - This plot simply illustrates the periods of the mission when the source is visible from Herschel.
- Visibility constraint vs. date.
    - This plot, divided into four time periods for clarity, indicates potential problems with observing the source at that epoch. The Y-axis level indicates the constraint with the following code:-
        - 0 Source not visible
        - 1 Source visible with no warnings
        - 2 Within 10° of Galactic centre
        - 3 Within 2° of Orion
        - 4 Within 2° of τ-Aur
        - 5 Within 2° of Ophiuchus
        - 6 Within 2° of LMC
        - 7 Within 2° of Jupiter
        - 8 Within 2° of Saturn
        - 9 Within 2° of Uranus
        - 10 Within 2° of Neptune
        - 11 Within 2° of Mars
        - 12 Within 5° of Galactic plane
- Velocity vs. date.

- This plot shows the source velocity, in arcsec/Hr, during the visibility periods.

Visibility plots are only shown for the primary sources in this document, but plots for all sources are embedded in the MS Project file.

8 Primary Calibration Sources

8.1 Neptune

Neptune is the proposed primary calibration source for SPIRE. The expected flux is ideal for SPIRE. But there are absorption features (broad PH_3, CO and HCN lines) in all bands, and these need to be well understood and modelled.

8.1.1 Visibility

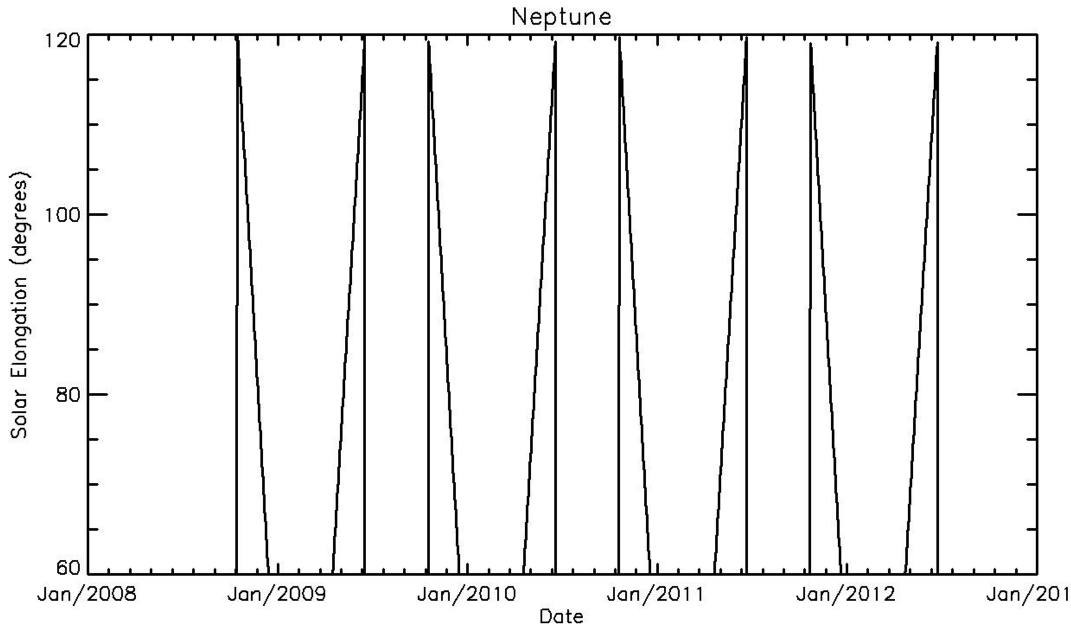

Figure 1 Periods for which Neptune is observable by Herschel (60°< solar elongation<120°)

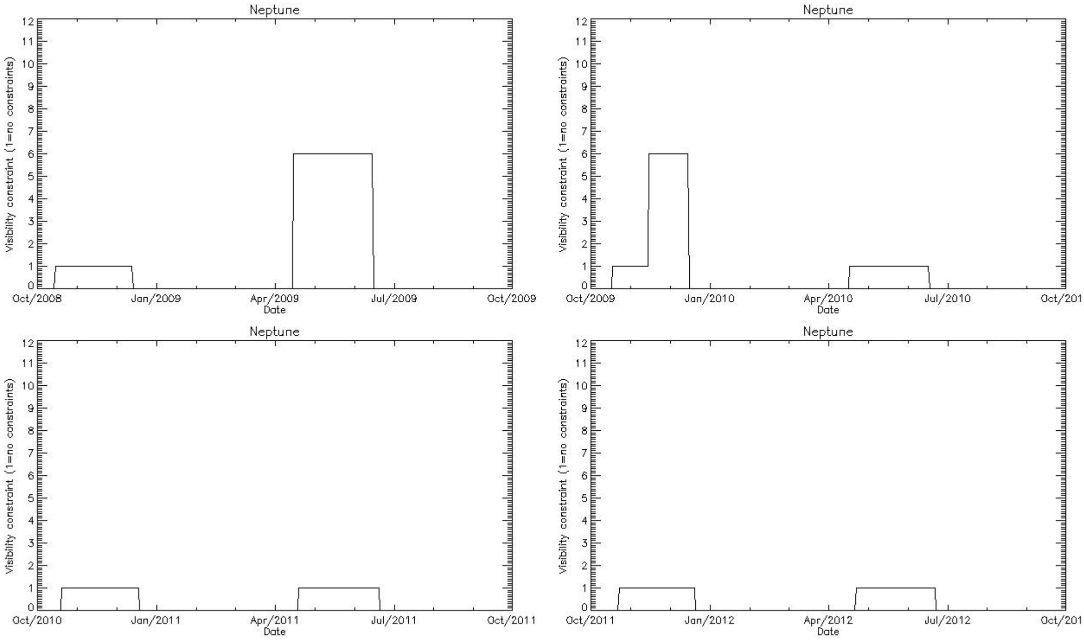

Figure 2 Constraints on observability periods.

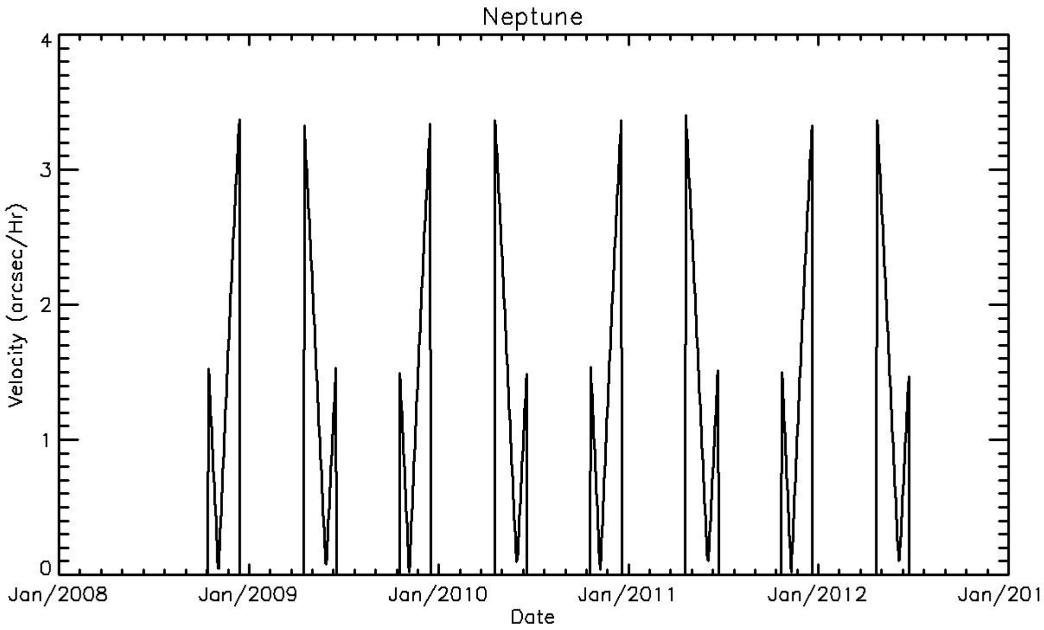

Figure 3 Source velocity during observable periods

8.1.2 Neptune flux prediction

Predicted brightness temperatures and derived flux ranges in the SPIRE bands are tabulated below (Moreno – Hcal workshop, Encrenaz et al).

Table 1 Flux range for Neptune during Herschel mission

Band	PSW	PMW	PLW
T_B(K)	63	64	70
$S_\upsilon$max (Jy)	268	119	50
$S_\upsilon$min (Jy)	259	115	48

Accurate flux predictions for the epochs of observability will be supplied by Raphael Moreno. The minimum and maximum flux values listed in table 1 are derived from the expected range in solid angle of the source.

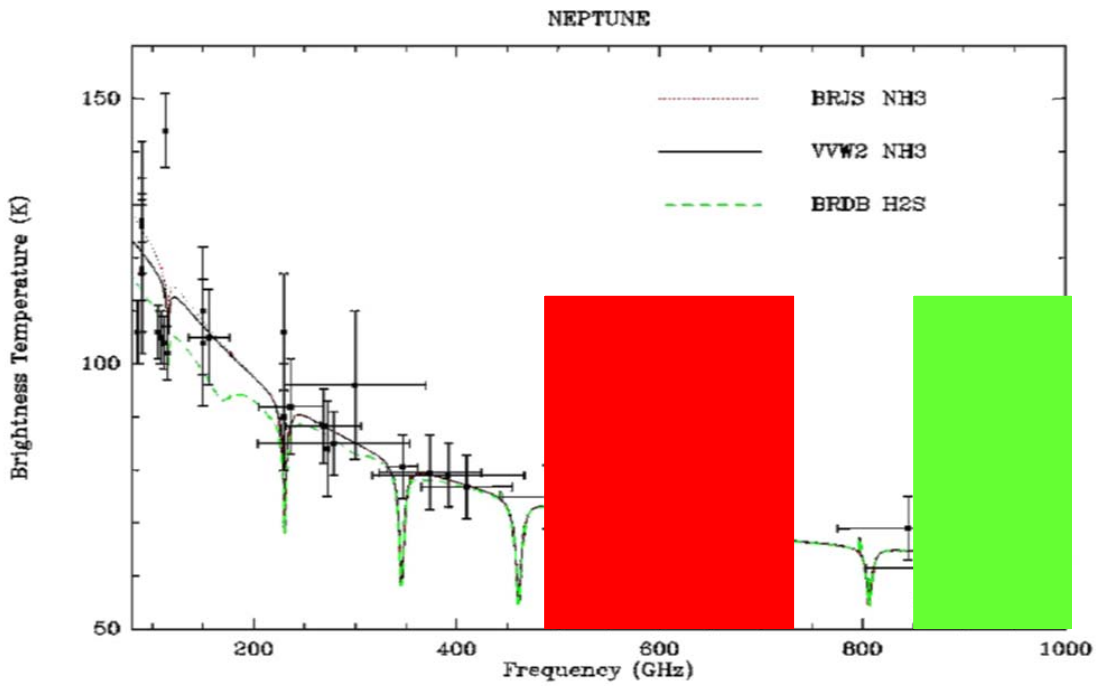

Figure 4 Neptune model fit – from Encrenaz & Moreno. Coloured boxes indicate SPIRE bands.

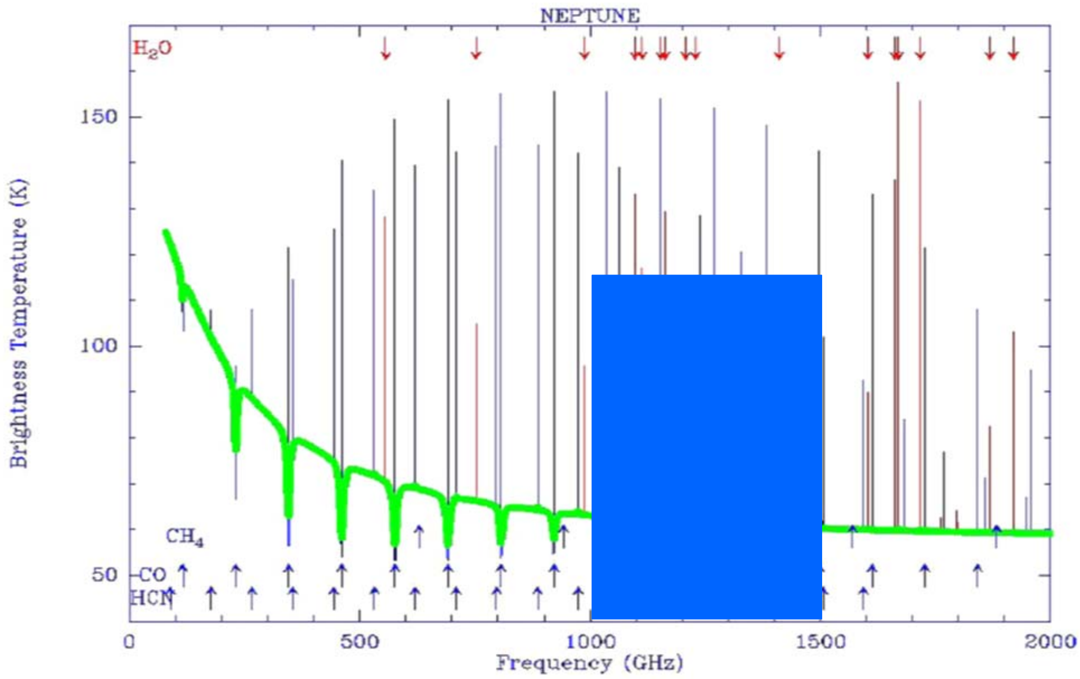

Figure 5 Neptune model fit – from Encrenaz & Moreno. Blue box indicates SPIRE PSW band.

8.1.3 Model fidelity

TBC

8.1.4 Variability

TBC

8.1.5 Calibration accuracy

TBC

8.2 Uranus

Uranus is a useful calibration source for SPIRE. Although it will be very bright in the SPIRE bands, any non-linearity effects induced in the detectors are well understood, and can be easily corrected for.

8.2.1 Visibility

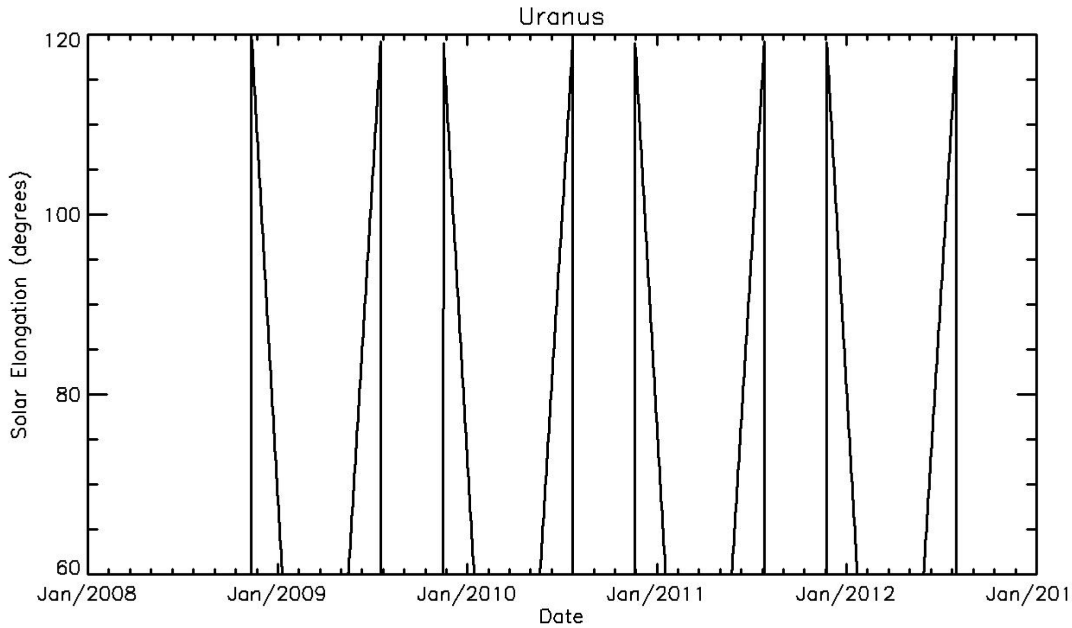

Figure 6 Periods for which Neptune is observable by Herschel (60°< solar elongation<120°)

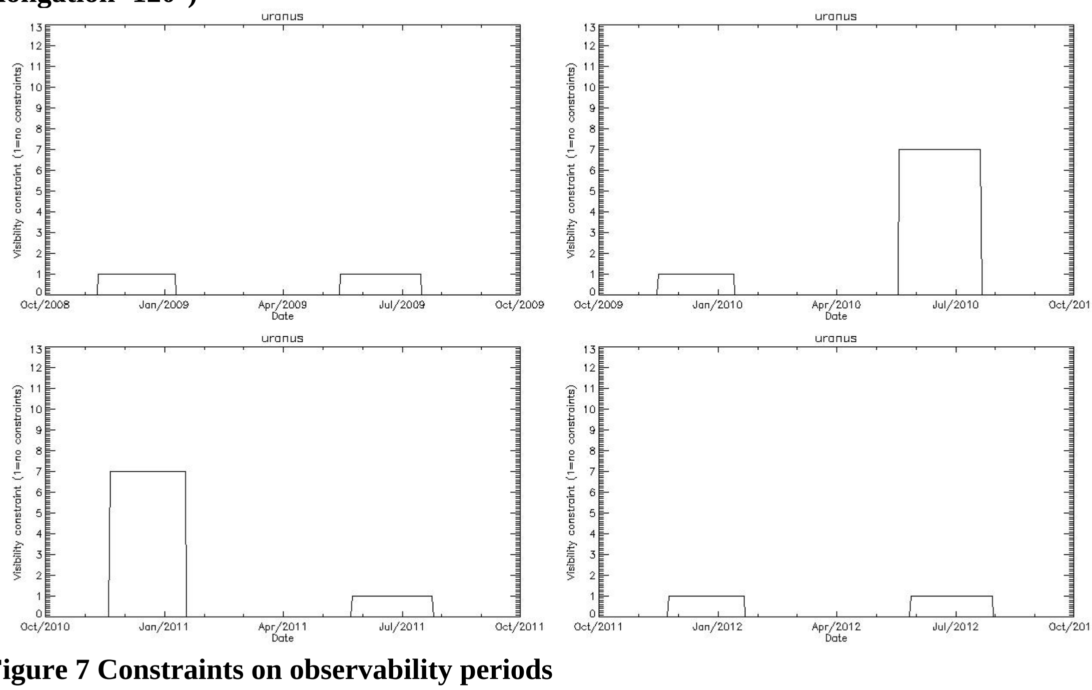

Figure 7 Constraints on observability periods

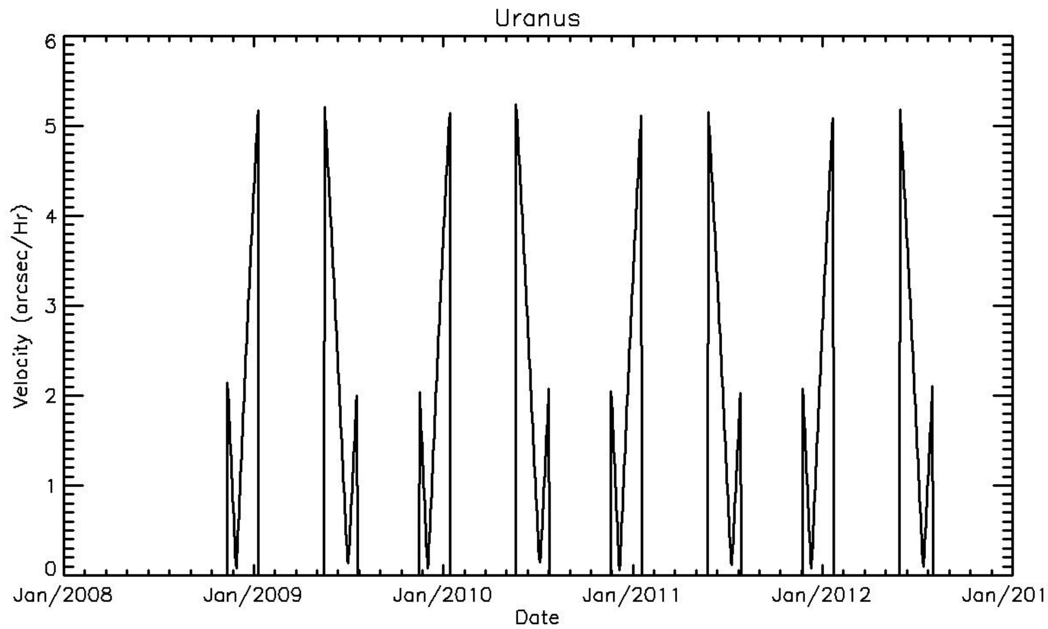

Figure 8 Source velocity during observability periods

8.2.2 Flux prediction

Predicted brightness temperatures and derived fluxes in the SPIRE bands are tabulated below (Encrenaz & Moreno).

Table 2 Flux range for Uranus during Herschel mission

Band	PSW	PMW	PLW
T_B(K)	63	67	72
$S_\upsilon$max (Jy)	792	364	149
$S_\upsilon$min (Jy)	641	295	121

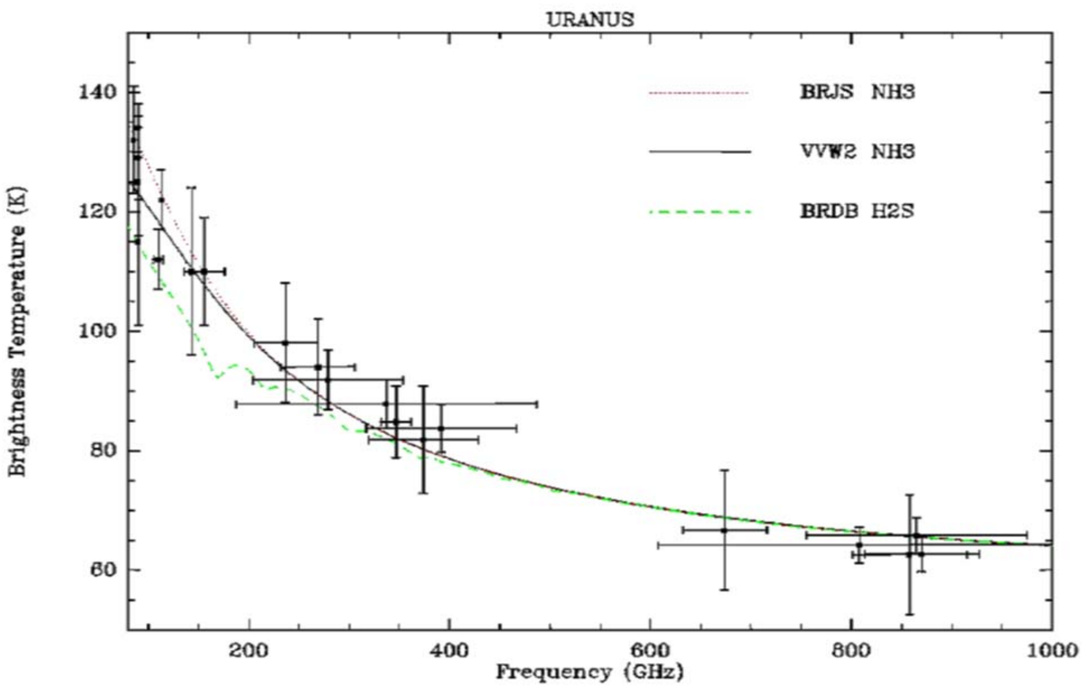

Figure 9 Uranus model fit – from Encrenaz & Moreno

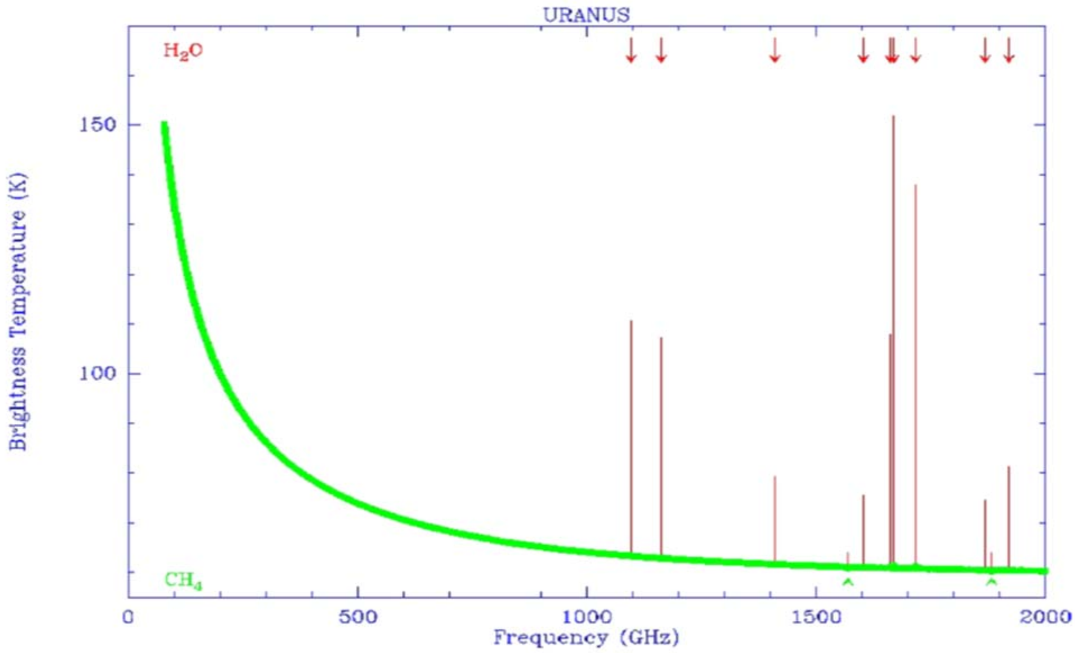

Figure 10 Uranus model fit – from Encrenaz & Moreno

8.2.3 Model fidelity

8.2.4 Variability

8.2.5 Calibration accuracy

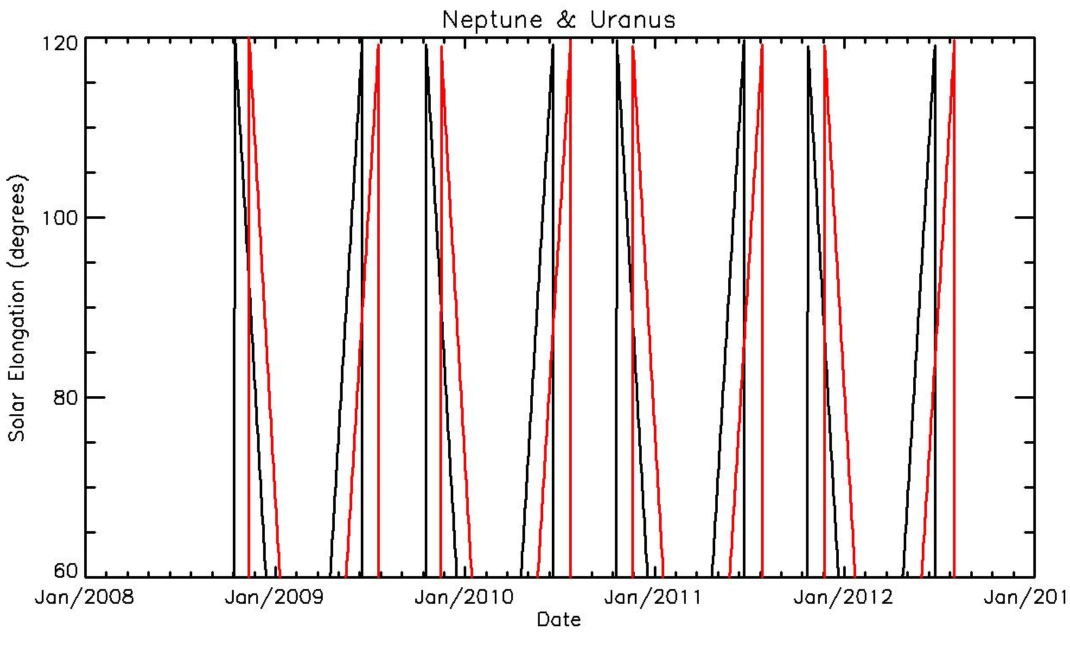

Figure 11 Periods during which primary sources are visible.

9 Secondary Calibration Sources

9.1 Asteroids

A list of fifty five asteroids have been selected as potential calibration sources for SPIRE. Of these, eleven have been flagged as "primary" asteroids (quality A or A-B). This status reflects the quality of the input parameters available for the thermo-physical model developed by Mueller & Lagerros (ref). Primary asteroids are highlighted in green in Table 3.

Table 3 Asteroid calibration sources for SPIRE.

#	PH #	Name	Quality	Comments
1	0	Ceres	A	
2	1	Pallas	B	
3	2	Juno	A	
4	3	Vesta	A-B	
6	5	Hebe	A	
7	6	Iris	D	
8	7	Flora	B	
9	8	Metis	C	
10	9	Hygeiea	B-C	
12	11	Victoria	B	
17	16	Thetis	D	
18	17	Melpomene	B	
19	18	Fortuna	D	
20	19	Massalia	B	
21	20	Lutetia	B	
23	21	Thalia	B	
24	22	Themis	B	
28	23	Bellona	B	
29	24	Amphitrite	B	
31	25	Euphrosyne	B-C	
37	26	Fides	B-C	
40	27	Harmonia	B-C	
41	28	Daphne	B-C	
42	29	Isis	B	
47		Aglaja	A-B	
48	31	Doris	B	
52	32	Europa	A	
54		Alexandra	B	
56		Melete	B-C	
65	33	Cybele	A	
69		Hesperia	B	
85		Io	B	
88		Thisbe	A-B	
93		Minerva	A-B	
94		Aurora	B	
106		Dione	C	
165		Loreley	B-C	
173		Ino	B-C	
196		Philomela	B-C	
230		Athamantis	A-B	
241		Germania	B-C	
283		Emma	B-C	
313		Chaldaea	B	
334		Chicago	C	
360		Carlova	D	
372		Palma	B-C	
423		Diotima	A	
451		Patientia	C	
471		Papagena	B	
505		Cava	B	
511		Davida	B	
532	34	Herculina	C	
690		Wratislavia	B	
704		Interamnia	B	
776		Berbericia	B	

9.1.1 Asteroid flux estimation

At the Herschel Calibration Workshop in Madrid (February 2008), it was agreed that Thomas Mueller (MPE) would provide the following:-

- Simple flux predictions (modified STM) for all 55 asteroids at 70,160,250,350,500 and 3000 microns for full Herschel mission (L2-centric, time resolution 1 day). This will be available for planning purposes via a web-page interface. This will include confusion noise estimation at 100 and 160 microns along the apparent sky paths, and warnings of close encounters between asteroids and planets. Results will be in ecliptic, galactic, RA/Dec, and sun-centric coordinates.
- For the final calibration, post observation, on request:-
    - SED prediction for a given epoch (thermo-physical model)
    - Thermal lightcurve prediction for a given wavelength
    - Quality assessment for individualproducts
    - Products delivered as FITS files or ASCII tables

9.1.2 Asteroid visibility – need to update for new primary list

Using just the primary recommended asteroids, there is a 2 month period of the mission from late July to late September 2009 where no preferred source is available.

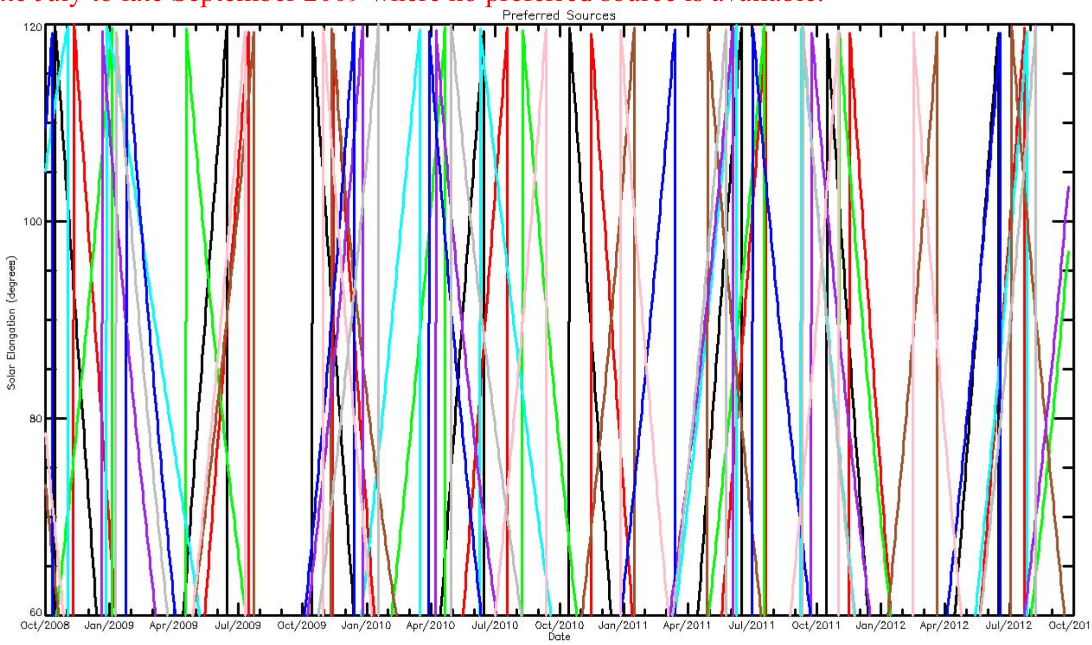

Figure 12 Visibility for preferred calibration targets. Key: Black=Neptune, Red=Uranus, Green=Ceres, Cyan=Pallas, Brown=Juno, Purple=Vesta, Blue=Hygeiea, Pink=Cybele, Grey=Herculina

9.2 Planetary nebulae

9.2.1 CRL 618

This source is the most popular secondary calibrator in use at the JCMT (Jenness et al. (MNRAS – get ref), Sandell (2001), Sandell (1994). It is essentially point-like (8" at 450µm, Jenness et al.) in the SPIRE 250µm beam, with no evidence for extended structure out to 20" radius (the SCUBA chop throw). Knapp, Sandell & Robson (1993) indicate a possibility of source variability in the mm region, but there is no obvious variability in the SCUBA-850 channel over a four year period.
The 450µm flux (for a 40" aperture) for this source is 12.1±2.2 Jy (Jenness et al.)

9.2.2 CRL 2688

Also a secondary JCMT calibrator, this source is slightly more extended than CRL 618, having a "source size" of 9.5" (Jenness et al.).
The 450µm flux (for a 40" aperture) for this source is 30.9±3.8 Jy (Jenness et al.)

9.3 T-Tauri stars

9.3.1 HL Tau

HL Tau has a compact, unresolved (by JCMT) core, but the star is associated with faint extended emission out to a FWHM of ~8" at 450µm. For 450 µm, the amount of extended emission is uncertain, because JCMT data shows variation of the integrated error lobe of the order of 15 – 20 % for benign conditions. However, the corresponding estimates are about 2.3 Jy and 3.6 Jy for 60 and 120" apertures, respectively. Most of the extended emission is relatively compact and at low level, but it is recommended not to observe HL Tau with JCMT chop throws shorter than 60".

9.4 Stellar sources

We intend to use selected sources from the list produced by Martin Groenewegen (internal communication). These sources should ideally have a 500µm flux >100mJy, with a predicted flux error <10% (TBC). In reality, the flux errors are likely to be of the order ~20% due to uncertainties in the extrapolation of the models to the SPIRE wavelengths, and lack of other sub-mm observational data.

There are 2 SPIRE AOTs of relevance: The point-source AOT which takes 579 sec and results in an rms noise of 1.4, 1.6, 1.3 mJy at 250, 350, 500 micron, respectively, and the small-map AOT which takes 687 sec and leads to a noise level of 4.7, 6.3, 5.3 mJy. These noise levels should be added in quadrature to the cirrus confusion noise levels mentioned below. The stellar fluxes have been derived from extrapolation using simple model atmospheres fitted to known ISO or IRAS fluxes. The accuracy should be 20% or so, but in any case sufficient to check the feasibility of SPIRE observations. HSPOT was used to get the background and confusion noise numbers. The predicted fluxes, backgrounds and confusion noise levels are listed in Table 4. It shows that at least 5 stars, and with some more effort also gamma Dra are sufficiently bright to lead to good S/N observations. If required and essential even Sirius is not out of the question if the AOT is executed with a repetition factor of ~10 (taking 1 hour for the point-source AOT).

Table 4 Predicted fluxes and noise levels of brightest stellar standards.

Name	BG at 100 μm (MJy/sr)	flux (mJy)	cirrus confusion noise (mJy/pixel)	cirrus confusion noise (mJy/pixel)
γ-Cru	52			
250 micron		1390	63	70 micron = 0.44
350		640	51	110 micron = 5.2
500		340	28	170 micron = 37.
α- Boo	6.3			
250 micron		1100	4.6	70 micron = 0.02
350		500	5.6	110 micron = 0.24
500		260	4.5	170 micron = 1.0
α-Tau	42			
250 micron		1000	37	70 micron = 0.26
350		460	30	110 micron = 3.1
500		240	17	170 micron = 22.
β-Peg	10.1			
250 micron		580	5.3	70 micron = 0.02
350		270	6	110 micron = 0.32
500		140	4.6	170 micron = 1.85
β-And	7.5			
250 micron		420	4.6	70 micron = 0.02
350		190	5.6	110 micron = 0.25
500		100	4.5	170 micron = 1.21
γ-Dra	5.8			
250 micron		240	4.7	70 micron = 0.02
350		110	5.6	110 micron = 0.25
500		60	4.5	170 micron = 1.17
Sirius	35			
250 micron		230	34	70 micron = 0.23
350		110	28	110 micron = 2.8
500		50	15	170 micron = 19.9

10 Line sources

Selection of line sources for the spectrometer calibration is still in progress, at the time of this document issue. The rest of this section (green text) is a technical note from Ed Polehampton, which summarises the requirements, followed by a recent telecon summary (blue).
****

Calibration sources are needed to,

calibrate the wavelength scale
monitor the flux calibration of lines
verify the spectral resolution
examine the interferogram fringe contrast
check narrow band properties

This means we require some fairly bright sources that have,

Many discrete, strong lines
Well defined and previously measured line fluxes
Single strong lines at different wavelengths in different sources

SPIRE Wavelength Calibration

The SPIRE wavenumber scale is generated by the FFT of the measured interferogram signal. An accurate wavenumber axis requires an accurate *Optical Path Difference* (*OPD*) axis in the interferogram.

We actually measure *Mechanical Path Difference* (*MPD*) rather than OPD, and so there must be a calibration to convert from one to the other,

$$OPD = f \times MPD$$

where f~4, but depends on the distance off axis from the central pixel.

SPIRE Instrument Line Shape

The spectral resolution of each spectrum is set by the distance that the mirror is scanned and the instrumental line shape should be a Sinc function. In all lab tests the line shape can be accurately fitted with the theoretical Sinc function. However, this must be verified in flight using unresolved spectral lines.

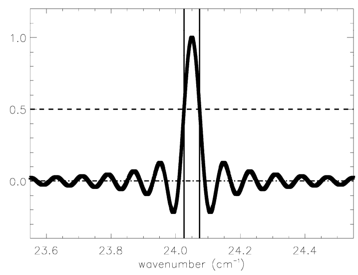

Sources

ISO LWS used atomic and ionic lines for their flux calibration. This is because these lines are strong, narrow and available in many sources. However, for SPIRE we only have 3 main ionic lines across the band:
NII at 205.2 µm
CI at 370.4 µm
CI at 609.1 µm

We also have CO lines from J=5-4 to J=13-12 and water lines.

Water lines

Ortho	**Wavelength**
1_01-1_10	538.289
3_03-3_12	273.193
2_12-3_12	259.982
3_12-3_21	257.795
Para	
0_00-1_11	269.272

1_11-2_02	303.456
2_02-2_11	398.643

CO Lines	**Wavelength**
4-3	650.25
5-4	520.231
6-5	433.556
7-6	371.65
8-7	325.225
9-8	289.12
10-9	260.24
11-10	236.613
12-11	216.927
13-12	200.272

The CO lines provide an even comb of lines across the SPIRE band and in many sources will be strong.

CO lines up to *J*=7-6 have been observed from the ground at sub-mm telescopes such as the CSO in several sources. Higher *J* CO lines have been observed in fewer sources. For example, OMC-1: Marrone et al. 2004, 612, 940 ApJ measured CO *J*=9-8 with an 84" beam. CONDOR at APEX measured *J*=13-12 in Orion.

For most objects we will need to find modelled values for CO fluxes between the ground based measurements and the ISO LWS measurements.

Before a star develops an HII region, CI becomes enhanced with respect to CO.
On the AGB, CO is stronger than CI. Therefore AGB stars might be better for a comb of many lines.
Evolved objects have stronger CI – ie. PPNe and HII regions

[NII] Line at 205 microns

Observations by COBE showed that the NII line at 205 μm was the second strongest line after CII in the wavenumber range 1–80 cm^{-1} (Wright et al. 1991). It is approximately 1/10 as strong as CII in the average galactic spectrum. The ratio of NII line flux 122/205 is predicted to be lowest in low density HII regions (~3:1), compared to 10:1 in high density regions. In the average COBE galactic spectrum the ratio is 1.6:1.

NII has been detected in the HII region G333.6–0.2 by Colgan et al. (1993), with a flux of 4.4×10^{-14} Wm^{-2} against a continuum of 4000 Jy using the KAO. It has also been detected towards the Carina nebula by Oberst et al. (2006) with a flux of 1.03×10^{-14} Wm^{-2} in the AST/RO 54" beam, and M82 by Petuchowski et al. (1994) using the KAO with a flux of 7.1×10^{-15} Wm^{-2}.

Petuchowski, S. J.; Bennett, C. L.; Haas, Michael R.; Erickson, Edwin F.; Lord, Steven D.; Rubin, Robert H.; Colgan, Sean W. J.; Hollenbach, D. J.
1994ApJ...427L..17

Telecon about FTS spectral line calibration sources, 11 March 2008

Ed Polehampton
Tanya Lim
Jean-Paul Baluteau
David Naylor
Peter Davis
Trevor Fulton
Nanyao Lu
Bernhard Schulz
Sarah Leeks

The decisions made were:
========================

* Use an extended line source for Obliquity correction measurement so all detectors are measured at the same time. Aim for S/N of 20 in lines.

* Check line flux calibration using AGB star CO lines as reference spectra

* Make 2 full beam maps: centre detector and one off-axis. Other detectors to be done using cross scans. Low spectral resolution will be used.

* Schedule a quick test of BSM calibration for the spectrometer to confirm it is same as photometer

Next steps:
===========
- Calibration Steering group will decide on common AGB star CO line sources for 3 instruments
- Ed will check with Jean-Paul about extended line sources for obliquity correction
- PV plan will be updated with the above tests.

11 Pointing calibration sources for SPIRE

Pointing calibration sources for SPIRE have been selected from a sub-set of the JCMT and SEST pointing catalogues. The objects in these catalogues are mainly QSO or BL Lac objects. Additionally, two special sources have been selected for focal plane spatial calibration.

11.1 Flux estimation

It should be noted that these sources are highly variable, and in each case, the lowest quoted flux has been used. SPIRE fluxes for the pointing sources have been derived from the lowest quoted 230 GHz fluxes for the SEST sources, and from the lowest 850 μm fluxes for the JCMT sources. To estimate the flux in the SPIRE bands, I extrapolated the SEST and JCMT fluxes to the SPIRE bands assuming a spectral index of -0.7. This pessimistic spectral index was chosen assuming synchrotron emission only, with no contribution from a dust component. In reality, one would expect a significant contribution from dust for many of these sources. So in all cases, the SPIRE flux estimates quoted should be a lower limit.

11.2 Source selection

Sources were selected from the two catalogues based on their predicted 250 μm flux. For a pointing calibration observation, we require a source which is sufficiently bright at 250 μm to give a good signal-to-noise ratio (S/N) in a short observation. We have selected sources which should give a S/N > 100 in a 256 second (time on-source) point-source observation. This equates to a 250 μm flux >150 mJy.

11.3 Special sources – focal plane geometry calibration

Two special sources have been identified which have special utility as focal-plane geometry calibrators. These are Cygnus-A (Robson et al., Wright et al.) and DG Tau/DG TauB (ref.…). Cygnus-A forms a triple source system, with the central core separated from each of the two radio lobes by approximately 1'. DG Tau/DG TauB is a double source, separated by ~57". More sources to be added…..

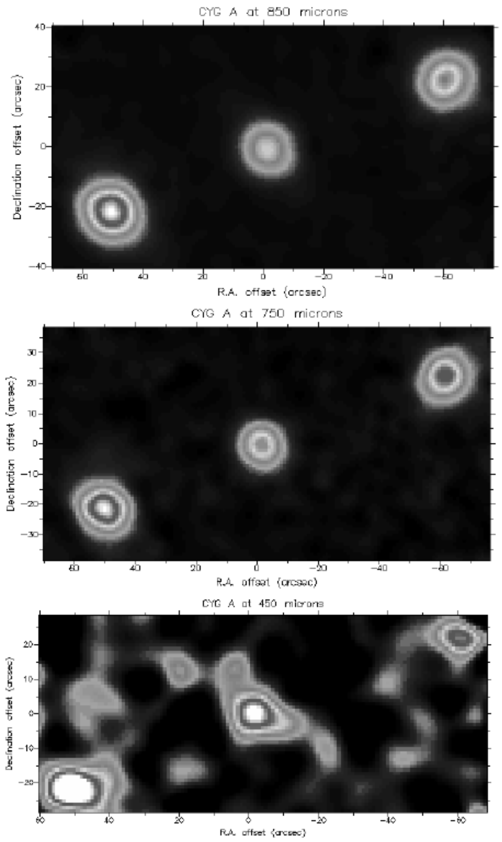

Figure 13 Sub-mm maps of Cyg-A, from Robson et al., 1998

11.4 Pointing source list

	Catalogue	RA-J2000	DEC-J2000	Name	F250	F350	F500
		"h:m:s"	"d:m:s"		mJy	mJy	mJy
95	SEST	12 29 06.41	+02 03 05.2	B1226+023	4628	5857	7518
100	SEST	12 56 11.17	-05 47 21.6	B1253-055	4155	5258	6750
135	SEST	18 00 30.43	-24 04 01.5	B1757-240	3519	4454	5717
104	SEST	13 25 27.61	-43 01 08.8	B1322-428	2897	3667	4707
142	JCMT	19 24 51.056	- 29 14 30.12	1921-293	1698	2149	2759
99	JCMT	12 56 11.167	- 05 47 21.52	3C279	1444	1827	2345
169	JCMT	22 53 57.748	+ 16 08 53.56	2251+158	1444	1827	2345
71	JCMT	08 54 48.875	+ 20 06 30.64	OJ287	1401	1773	2276
166	JCMT	22 32 36.409	+ 11 43 50.90	2230+114	1401	1773	2276
43	SEST	04 55 50.77	-46 15 58.7	B0454-463	1147	1452	1863
105	JCMT	13 37 39.783	- 12 57 24.69	1334-127	1019	1290	1655
85	SEST	11 18 57.30	+12 34 41.7	B1116+128	1019	1289	1655
50	JCMT	05 38 50.362	- 44 05 08.94	PKS0537	977	1236	1586

29	JCMT	03 19 48.160	+ 41 30 42.10	3C84	934	1182	1517
96	JCMT	12 29 06.700	+ 02 03 08.60	3C273	892	1128	1448
17	SEST	02 10 46.20	-51 01 01.9	B0208-512	824	1043	1339
132	JCMT	17 43 58.856	- 03 50 04.62	1741-038	807	1021	1311
33	JCMT	03 59 29.747	+ 50 57 50.16	0355+508	764	967	1242
36	JCMT	04 23 15.801	- 01 20 33.07	0420-014	764	967	1242
97	JCMT	12 30 49.423	+ 12 23 28.04	VirgoA	764	967	1242
46	SEST	05 06 44.00	-61 09 41.0	B0506-612	743	940	1207
72	SEST	09 09 10.09	+01 21 35.6	B0906+015	739	935	1200
53	SEST	06 04 25.17	-42 25 30.0	B0602-424	685	866	1112
59	JCMT	07 21 53.448	+ 71 20 36.36	0716+714	679	860	1104
92	JCMT	11 53 24.467	+ 49 31 08.83	1153+495	637	806	1035
128	JCMT	16 42 58.810	+ 39 48 36.99	3C345	637	806	1035
51	SEST	05 38 50.37	-44 05 09.0	B0537-441	635	804	1032
34	SEST	04 03 53.77	-36 05 01.5	B0402-362	541	685	879
56	SEST	06 35 46.55	-75 16 16.8	B0637-752	528	669	859
23	JCMT	02 37 52.406	+ 28 48 08.99	0234+285	510	645	828
1	JCMT	00 06 13.893	- 06 23 35.33	0003-066	467	591	759
11	JCMT	01 36 58.595	+ 47 51 29.10	0133+476	467	591	759
131	JCMT	17 33 02.706	- 13 04 49.55	1730-130	467	591	759
161	JCMT	22 02 43.291	+ 42 16 39.98	BLLAC	467	591	759
164	JCMT	22 25 47.259	- 04 57 01.39	2223-052	467	591	759
55	JCMT	06 09 40.950	- 15 42 40.67	0607-157	425	537	690
65	JCMT	07 57 06.643	+ 09 56 34.85	0754+100	425	537	690
75	JCMT	09 27 03.014	+ 39 02 20.85	0923+392	425	537	690
174	SEST	23 48 02.61	-16 31 12.0	B2345-167	411	521	668
98	SEST	12 46 46.80	-25 47 49.3	B1244-255	408	517	663
15	SEST	02 04 50.41	+15 14 11.0	B0202+149	405	512	658
146	SEST	19 57 59.82	-38 45 07.0	B1954-388	392	496	637
116	JCMT	15 17 41.813	- 24 22 19.48	1514-241	382	484	621
137	JCMT	18 06 50.681	+ 69 49 28.11	1807+698	382	484	621
91	SEST	11 52 17.19	-08 41 04.0	B1149-084	379	480	616
67	SEST	08 25 50.33	+03 09 24.5	B0823+033	379	479	615
6	SEST	01 08 38.75	+01 34 58.9	B0106+013	369	467	599
119	SEST	15 49 29.44	+02 37 01.2	B1546+027	358	453	582
88	SEST	11 47 01.34	-38 12 11.5	B1144-379	357	451	579
139	SEST	18 33 39.89	-21 03 39.8	B1830-211	345	437	560
48	JCMT	05 30 56.417	+ 13 31 55.15	0528+134	340	430	552
60	JCMT	07 30 19.112	- 11 41 12.60	0727-115	340	430	552
127	JCMT	16 35 15.493	+ 38 08 04.50	1633+382	340	430	552
167	SEST	22 35 13.23	-48 35 58.8	B2232-488	324	410	527
10	SEST	01 32 43.48	-16 54 48.5	B0130-171	305	386	495
81	JCMT	10 58 29.605	+ 01 33 58.82	1055+018	297	376	483
141	JCMT	19 11 09.653	- 20 06 55.11	1908-202	297	376	483
149	JCMT	20 07 44.945	+ 40 29 48.60	2005+403	297	376	483
170	JCMT	22 58 05.963	- 27 58 21.26	2255-282	297	376	483
82	SEST	10 58 43.31	-80 03 54.1	B1057-797	288	364	468
87	SEST	11 30 07.05	-14 49 27.4	B1127-145	286	363	465
83	SEST	11 03 52.22	-53 57 00.7	B1101-536	272	344	441
3	SEST	00 51 09.49	-42 26 33.3	B0048-427	269	340	437
30	SEST	03 34 13.65	-40 08 25.1	B0332-403	266	336	432

107	SEST	13 57 04.43	+19 19 07.4	B1354+195	260	329	422
69	SEST	08 36 39.25	-20 16 58.8	B0834-201	256	324	416
24	JCMT	02 38 38.930	+ 16 36 59.27	0235+164	255	322	414
44	JCMT	04 57 03.179	- 23 24 52.02	0454-234	255	322	414
62	JCMT	07 39 18.034	+ 01 37 04.62	0736+017	255	322	414
120	JCMT	15 50 35.269	+ 05 27 10.45	1548+056	255	322	414
122	JCMT	16 13 41.064	+ 34 12 47.91	1611+343	255	322	414
136	JCMT	18 00 45.684	+ 78 28 04.02	1803+784	255	322	414
112	SEST	14 54 27.60	-37 47 34.7	B1451-375	251	317	407
84	SEST	11 07 08.70	-44 49 07.7	B1104-445	236	299	384
89	SEST	11 47 33.63	-67 53 41.8	B1145-676	233	295	378
5	SEST	01 06 45.11	-40 34 20.0	B0104-408	232	294	377
155	SEST	21 23 44.52	+05 35 22.2	B2121+053	227	287	369
79	SEST	10 48 06.62	-19 09 35.8	B1045-188	226	286	367
12	SEST	01 37 38.35	-24 30 53.9	B0135-247	223	282	362
19	SEST	02 17 48.96	+01 44 49.6	B0215+015	223	282	362
150	SEST	20 09 25.39	-48 49 53.8	B2005-489	220	278	357
123	SEST	16 17 18.06	-58 48 09.7	B1613-586	218	275	353
173	SEST	23 29 17.70	-47 30 19.1	B2326-477	217	274	352
18	JCMT	02 17 30.813	+ 73 49 32.62	0212+735	212	269	345
47	JCMT	05 22 57.985	- 36 27 30.85	0521-365	212	269	345
61	JCMT	07 38 07.394	+ 17 42 19.00	0735+178	212	269	345
76	JCMT	09 58 47.245	+ 65 33 54.82	0954+658	212	269	345
103	JCMT	13 16 07.986	- 33 38 59.17	1313-333	212	269	345
125	JCMT	16 25 46.892	- 25 27 38.33	1622-253	212	269	345
138	JCMT	18 24 07.068	+ 56 51 01.49	1823+568	212	269	345
147	JCMT	20 00 57.090	- 17 48 57.67	1958-179	212	269	345
158	JCMT	21 36 38.586	+ 00 41 54.21	2134+004	212	269	345
160	JCMT	21 58 06.282	- 15 01 09.33	2155-152	212	269	345
165	JCMT	22 29 40.084	- 08 32 54.44	2227-088	212	269	345
25	SEST	02 42 29.17	+11 01 00.7	B0239+108	211	267	343
154	SEST	21 09 33.19	-41 10 20.6	B2106-413	209	265	340
157	SEST	21 34 10.30	-01 53 17.2	B2131-021	206	261	335
113	SEST	15 04 24.98	+10 29 39.3	B1502+106	200	253	325
129	SEST	16 58 09.01	+07 41 27.6	B1655+077	198	251	322
111	SEST	14 27 56.35	-42 06 19.4	B1424-418	194	245	314
171	SEST	23 20 44.86	+05 13 50.0	B2318+049	190	241	309
145	SEST	19 37 16.30	-39 58 01.3	B1933-400	189	239	306
38	SEST	04 28 40.38	-37 56 19.7	B0426-380	179	227	291
37	SEST	04 24 42.36	-37 56 21.4	B0422-380	179	227	291
2	JCMT	00 50 41.318	- 09 29 05.21	0048-097	170	215	276
31	JCMT	03 39 30.938	- 01 46 35.80	0336-019	170	215	276
49	JCMT	05 32 38.998	+ 07 32 43.35	0529+075	170	215	276
54	JCMT	06 07 59.699	- 08 34 49.98	0605-085	170	215	276
70	JCMT	08 41 24.365	+ 70 53 42.17	0836+710	170	215	276
78	JCMT	10 37 16.080	- 29 34 02.81	1034-293	170	215	276
90	JCMT	11 50 19.212	+ 24 17 53.84	1147+245	170	215	276
102	JCMT	13 10 28.664	+ 32 20 43.78	1308+326	170	215	276
108	JCMT	14 15 58.817	+ 13 20 23.71	1413+135	170	215	276
115	JCMT	15 12 50.533	- 09 05 59.83	1510-089	170	215	276
143	JCMT	19 25 59.605	+ 21 06 26.16	1923+210	170	215	276

144	JCMT	19 27 48.495	+ 73 58 01.57	1928+738	170	215	276
151	JCMT	20 11 15.711	- 15 46 40.25	2008-159	170	215	276
153	JCMT	20 38 37.035	+ 51 19 12.66	2037+511	170	215	276
162	JCMT	22 03 14.976	+ 31 45 38.27	2201+315	170	215	276
168	JCMT	22 46 18.232	- 12 06 51.28	2243-123	170	215	276
124	SEST	16 17 49.27	-77 17 18.5	B1610-771	170	215	276
26	SEST	02 53 29.18	-54 41 51.5	B0252-549	169	214	274
27	SEST	03 03 50.63	-62 11 25.6	B0302-623	166	210	269
41	SEST	04 50 05.47	-81 01 02.2	B0454-810	162	205	263
4	SEST	00 58 46.58	-56 59 11.4	B0056-572	159	201	258
140	SEST	18 37 28.71	-71 08 43.5	B1831-711	156	197	253
42	SEST	04 53 14.65	-28 07 37.3	B0451-282	154	195	251
106	SEST	13 54 46.51	-10 41 02.7	B1352-104	154	195	251
172	SEST	23 23 31.95	-03 17 05.1	B2320-035	153	193	248
66	SEST	08 08 15.54	-07 51 09.8	B0805-077	150	190	244

12 References (incomplete)

Robson, E. I., Leeuw, L. L., Stevens, J. A., Holland, W. S., MNRAS, 301, 935-940 (1998)
Wright, M. C. H., Sault, R. J. ApJ, 402:546-549, 1993

Delete – included in project file….

Source	Window opens	Window closes	Duration	Flux
CRL2688	6/10/08	15/01/09	101	
	2/4/09	17/07/09	106	
	6/10/09	15/01/10	101	
	3/4/10	17/7/10	105	
	6/10/10	16/1/11	102	
	3/4/11	18/7/11	106	
	6/10/11	16/1/12	102	
	2/4/12	17/7/12	106	
	5/10/12	15/1/13	102	
	2/4/13	19/4/13	17	
CRL618	5/8/08	7/10/08	63	
	2/2/09	4/4/09	61	
	5/8/09	8/10/09	64	
	2/2/10	4/4/10	61	
	6/8/10	8/10/10	63	
	2/2/11	5/4/11	62	
	6/8/11	8/10/11	63	
	3/2/12	4/4/12	61	
	5/8/12	7/10/12	63	
	2/2/13	4/4/13	61	
IRC+10216	18/10/08	15/12/08	58	
	15/4/09	15/6/09	61	
	18/10/09	15/12/09	58	
	15/4/10	15/6/10	61	
	18/10/10	16/12/10	59	
	15/4/11	15/6/11	61	

	19/10/11	16/12/11	58	
	14/4/12	14/6/12	61	
	18/10/12	15/12/12	58	
	15/4/13	19/4/13	4	
To be completed…..				